Hypoxia-inducible factor 1-dependent expression of platelet-derived growth factor B promotes lymphatic metastasis of hypoxic breast cancer cells

Luana Schito[a,b,c], Sergio Rey[a,b], Marco Tafani[c], Huafeng Zhang[a,b], Carmen Chak-Lui Wong[a,b], Andrea Russo[d], Matteo A. Russo[c,e], and Gregg L. Semenza[a,b,f,g,h,i,j,1]

[a]Vascular Program, Institute for Cell Engineering, [b]McKusick Nathans Institute of Genetic Medicine, and Departments of [f]Pediatrics, [g]Medicine, [h]Oncology, [i]Radiation Oncology, and [j]Biological Chemistry, Johns Hopkins University School of Medicine, Baltimore, MD 21205; [c]Department of Experimental Medicine, Sapienza University of Rome, 00161 Rome, Italy; [d]Department of Surgical Pathology, Istituto di Ricovero e Cura a Carattere Scientifico Regina Elena, Istituti Fisioterapici Ospitalieri, 00161 Rome, Italy; and [e]Department of Cellular and Molecular Pathology, Istituto di Ricovero e Cura a Carattere Scientifico San Raffaele Pisana, 00163 Rome, Italy

Contributed by Gregg L. Semenza, August 14, 2012 (sent for review July 12, 2012)

Lymphatic dissemination from the primary tumor is a major mechanism by which breast cancer cells access the systemic circulation, resulting in distant metastasis and mortality. Numerous studies link activation of hypoxia-inducible factor 1 (HIF-1) with tumor angiogenesis, metastasis, and patient mortality. However, the role of HIF-1 in lymphatic dissemination is poorly understood. In this study, we show that HIF-1 promotes lymphatic metastasis of breast cancer by direct transactivation of the gene encoding platelet-derived growth factor B (PDGF-B), which has proliferative and chemotactic effects on lymphatic endothelial cells. Lymphangiogenesis and lymphatic metastasis in mice bearing human breast cancer orthografts were blocked by administration of the HIF-1 inhibitor digoxin or the tyrosine kinase inhibitor imatinib. Immunohistochemical analysis of human breast cancer biopsies demonstrated colocalization of HIF-1α and PDGF-B, which were correlated with lymphatic vessel area and histological grade. Taken together, these data provide experimental support for breast cancer clinical trials targeting HIF-1 and PDGF-B.

lymph node | orthotopic transplantation | triple-negative breast cancer

Metastasis is the major cause of mortality in breast cancer patients (1). Metastatic dissemination of cancer cells from the primary tumor may occur via blood vessels or lymphatic vessels (LVs). In breast cancer, the most clinically important predictor of distant organ metastasis and patient mortality is the presence and extent of axillary lymph node (LN) metastasis (1). Increased density of peritumoral and intratumoral LVs in breast cancer is significantly associated with LN metastasis and patient mortality (2). Two members of the vascular endothelial growth factor (VEGF) family, VEGF-C and VEGF-D, bind to VEGF receptor 3 on the surface of lymphatic endothelial cells (LECs) to stimulate growth of LVs (lymphangiogenesis) and cancer cell metastasis to LNs and distant sites (3, 4). VEGF-A, which primarily stimulates blood vessel angiogenesis, promotes lymphangiogenesis and LN metastasis, and members of the angiopoietin, FGF, insulin-like growth factor (IGF), and PDGF families also have been reported to promote lymphangiogenesis and metastasis (1, 5).

Intratumoral hypoxia is a common finding in breast cancer, and severe hypoxia [pO_2 <10 mm Hg (~1.5% O_2)] is associated with a significantly increased risk of metastasis and patient mortality (6). A major mechanism by which hypoxia promotes metastasis is through the hypoxia-inducible factors (HIFs), which activate the transcription of genes that play key roles in many critical aspects of cancer biology, including angiogenesis, metabolic reprogramming, epithelial–mesenchymal transition, and tissue invasion (7). HIFs are heterodimers composed of an O_2-regulated HIF-1α or HIF-2α subunit and a constitutively expressed HIF-1β subunit (7). HIF-1α is required for vascular metastasis from breast to lung in autochthonous (8) and orthotopic transplantation (9–11) mouse models. Clinical studies have found that increased HIF-1α levels in primary breast tumors are significantly associated with peritumoral LV density (12) and patient mortality (13). HIF-1α levels also were associated with LN metastasis in esophageal cancer (14). However, the mechanisms by which hypoxia stimulates LV density and LN metastasis in breast cancer are not known.

We addressed this issue using an orthotopic mouse model in which human breast cancer cells (BCCs) were injected into the mammary fat pad (MFP) of SCID mice. We previously demonstrated that stable transfection of MDA-MB-231 human BCCs with lentiviral vectors encoding shRNA to knock down the expression of HIF-1α (1αKD), HIF-2α (2αKD), or double knock down of both HIF-1α and HIF-2α (DKD) resulted in decreased primary tumor growth and lung metastasis compared with cells transfected with empty vector (EV) (9, 10). Treatment of tumor-bearing mice with digoxin, a drug that inhibits HIF activity, also impaired primary tumor growth and lung metastasis (10, 11). In the present study we have demonstrated effects of HIF loss of function on LN metastasis and LV density and have delineated molecular and cellular mechanisms underlying these effects.

Results

HIFs Regulate Peritumoral LV Density and LN Metastasis of BCCs. SCID mice received MFP injections of MDA-MB-231 BCCs, and the ipsilateral axillary LNs were harvested 24 d later. Histopathological examination of H&E-stained sections of the primary orthografts revealed a necrotic core in all tumor samples resulting from intratumoral hypoxia (15). H&E staining of axillary LNs showed distorted LN architecture, with loss of corticomedullary definition and hypochromatic nuclei, in mice bearing EV tumors, whereas LNs from mice bearing 1αKD, 2αKD, or DKD tumors presented a more preserved overall histology (Fig. S1*A*, *Upper*). Examination at higher magnification revealed that LNs from EV tumor-bearing mice contained cells characterized by anisocytosis, heterochromatic nuclei, and frequent mitoses (Fig. S1*A*, *Lower*). There was a decrease in the clinical histopathology score (HPS) of LNs from mice bearing 1αKD, 2αKD, or DKD tumors as compared with EV tumors (Fig. S1*B*). Because histopathological examination may underestimate LN metastasis (16), we performed immunohisto-

Author contributions: L.S. and G.L.S. designed research; L.S., S.R., M.T., H.Z., C.C.-L.W., and A.R. performed research; M.A.R. contributed new reagents/analytic tools; L.S., S.R., M.T., and G.L.S. analyzed data; and L.S. and G.L.S. wrote the paper.

The authors declare no conflict of interest.

[1]To whom correspondence should be addressed. E-mail: gsemenza@jhmi.edu.

See Author Summary on page 15991 (volume 109, number 40).

This article contains supporting information online at www.pnas.org/lookup/suppl/doi:10.1073/pnas.1214019109/-/DCSupplemental.

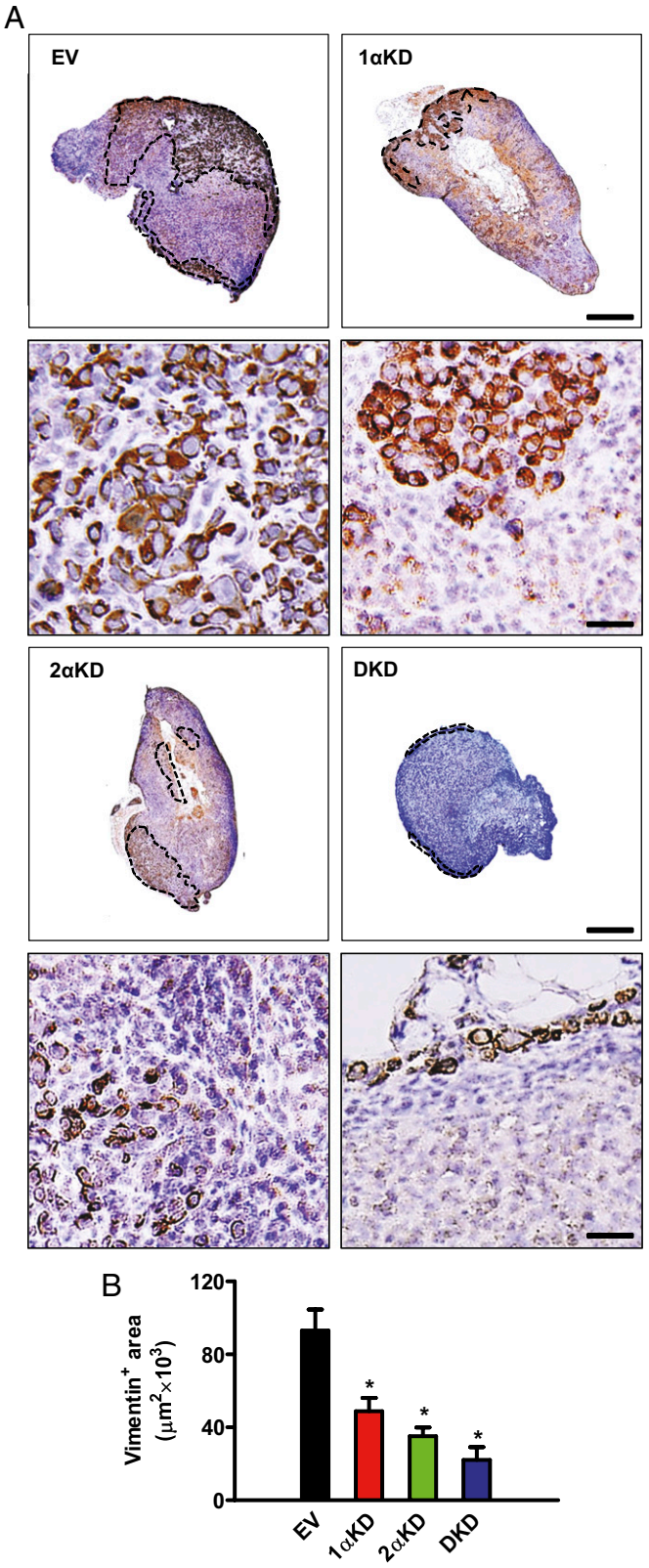

Fig. 1. HIF knockdown in breast cancer cells inhibits lymph node metastasis. MDA-MB-231 human BCCs, which were stably transfected with EV, or vectors encoding KD shRNAs directed against HIF-1α (1αKD), HIF-2α (2αKD), or both (DKD), were orthotopically transplanted into the MFP of SCID mice. (*A*) Axillary LNs ipsilateral to the tumors were harvested 24 d after transplantation, and sections were stained with an antibody specific for human vimentin [brown staining, which is cytoplasmic in high-magnification photomicrographs (*Lower Images*)]. (Scale bar, 50 μm.) Dotted lines in low-magnification photomicrographs (*Upper Images*) indicate the boundary between normal lymphoid cells and infiltrating vimentin-positive BCCs. (Scale bar, 500 μm.) (*B*) Digital image analysis of the vimentin-positive area. **P* < 0.05 vs. EV by Bonferroni test after one-way ANOVA. Data are expressed as mean ± SEM (*n* = 5 tumors each).

chemistry (IHC) on the same specimens with an antibody specific for human vimentin (Fig. S2*A*), expression of which is not regulated by HIFs (Fig. S2*B*). Most cells identified as LN metastatic foci by H&E were positive for human vimentin (Fig. 1*A*). Linear regression analysis showed a significant correlation ($r = 0.90$; $P < 0.001$) between HPS and the vimentin-positive area quantified by digital image analysis (Fig. S2*C*), which was decreased by 47% in 1αKD, 62% in 2αKD, and 76% in DKD LNs as compared with EV LNs (Fig. 1*B*).

Given our observation that LN metastasis of BCCs requires HIF and evidence that LV density is correlated with LN metastasis (1), we investigated whether HIF loss of function in BCCs had an effect on peritumoral LV density by performing IHC for podoplanin, which is expressed on LVs but not on blood vessels (3, 4). We found that LVs were located at the periphery of MDA-MB-231 tumors (Fig. 2*A*), as is commonly observed in human breast cancers and xenografts (1). LV density surrounding tumors composed of 1αKD, 2αKD, or DKD cells was reduced by 45%, 24%, and 27%, respectively, as compared with tumors composed of EV cells ($P < 0.05$). Tumor cells enter the lymphatic system by invading LVs (1). The luminal space of LVs from EV tumor-bearing mice was occupied by BCCs, whereas LVs in 1αKD, 2αKD, or DKD tumors seldom contained intravasated cells. IHC for podoplanin and vimentin performed on consecutive sections revealed intravasation of BCCs into LVs at the periphery of the primary tumors (Fig. 2*B*) and the presence of LVs in the subcapsular space of the ipsilateral axillary LNs (Fig. 2*C*). These findings suggest that HIF activity in BCCs is critical for LV density, LV invasion, and LN metastasis.

HIF-1 Regulates PDGF-B Levels in Human BCCs. To establish a molecular basis for the effect of HIFs on LN metastasis and LV density, we analyzed the expression of genes implicated in lymphangiogenesis (3–5). Exposure of MDA-MB-231 BCCs to hypoxia induced the expression of VEGF-A, BNIP3, and GLUT1 mRNAs, which are well-established HIF targets, as determined by reverse-transcription quantitative real-time PCR (qPCR) (Fig. 3*A*). HIF-1α and VEGF-C expression are associated with lymphangiogenesis in oral squamous cell carcinoma (17), but although VEGF-C mRNA was highly expressed in MDA-MB-231 cells, it was not induced by hypoxia, a result that is consistent with a previous report (18). VEGF-D expression is reduced in breast cancer biopsies and is inversely correlated with LN metastasis (19), and levels of VEGF-D mRNA were decreased in MDA-MB-231 cells under hypoxic conditions (Fig. 3*A*).

The presence or absence of HIF-1α and PDGF-B expression has been correlated in breast cancer biopsies (20), PDGF-B expression has been associated with LN metastasis in gastric cancer (21), and overexpression of PDGF-B in a tumor cell line increased lymphangiogenesis and lymphatic metastasis (22). Levels of PDGF-B mRNA, but not PDGF-A, PDGF-C, or PDGF-D mRNA, were significantly increased under hypoxic conditions (Fig. 3*A*). Further analysis revealed that mean PDGF-B mRNA levels increased 4.5-fold after 24 h and 5.5-fold after 48 h at 1% O_2 relative to MDA-MB-231 cells maintained at 20% O_2 (Fig. 3*B*, *Upper*). PDGF-B protein levels increased 2.2-fold after 48 h at 1% O_2 (Fig. 3*C*). Exposure of MDA-MB-231 cells to the prolyl hydroxylase inhibitor dimethyloxalylglycine (DMOG), which blocks HIF-1α and HIF-2α degradation (23), stimulated increased PDGF-B expression as determined by flow

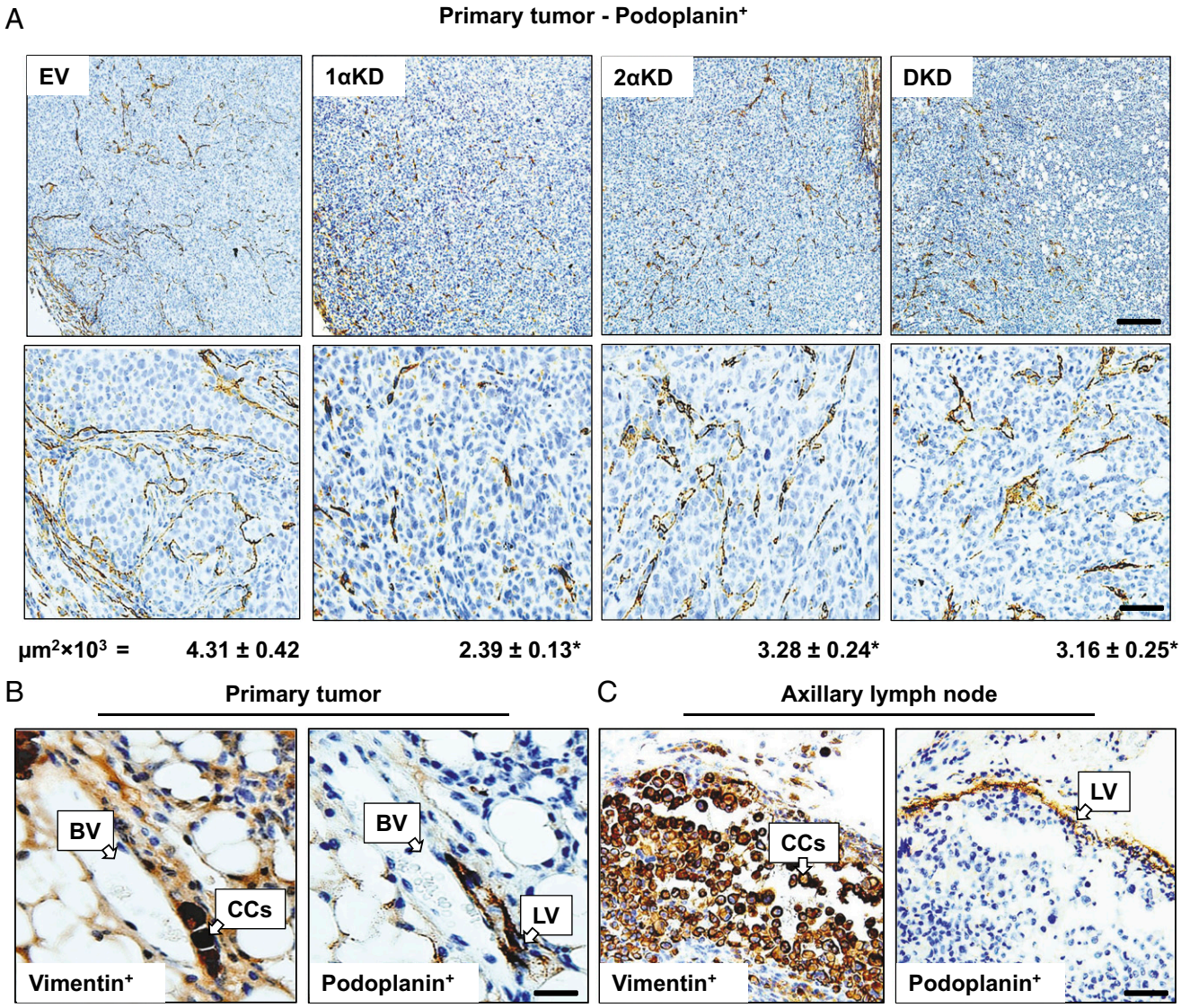

Fig. 2. HIF knockdown decreases the density of peritumoral lymphatic vessels. (*A*) IHC for podoplanin in primary breast cancer orthografts. LVs are stained brown and are visible at low (*Upper Row*; scale bar, 500 μm) and high (*Lower Row*; scale bar, 50 μm) magnification. Values under each column correspond to mean LV area digitally quantified for EV, 1αKD, 2αKD, or DKD tumors and expressed in thousands of square millimeters. (*B* and *C*) IHC of consecutive sections for human vimentin and podoplanin in the peritumoral region of MDA-MB-231 orthografts (*B*) or in axillary LNs (*C*). Invasion of cancer cells (CCs) into an LV was observed in the primary tumor, and CCs were observed in the vicinity of LVs in metastatic axillary LNs. Positive staining is brown; sections were counterstained with hematoxylin; note the absence of podoplanin staining of a blood vessel (BV). *$P < 0.05$ vs. EV by Bonferroni test after one-way ANOVA. Data are shown as mean ± SEM ($n = 5$).

cytometry (Fig. 3*D*). PDGF-B mRNA levels also were induced fourfold by hypoxia in MDA-MB-435, another metastatic BCC line (Fig. 3*B, Lower*). HIF DKD in MDA-MB-231 or MDA-MB-435 cells inhibited PDGF-B mRNA expression at 1% O_2 by 56% and 42%, respectively, relative to EV cells (Fig. 3*E*). To complement the genetic loss-of-function studies, MDA-MB-231 cells were exposed to digoxin, which had no effect on PDGF-B mRNA levels at 20% O_2 but inhibited hypoxic induction in a dose-dependent manner with an IC_{50} of 65.2 ± 1.2 nM and with complete inhibition at concentrations ≥100 nM (Fig. 3*F*).

***PDGFB* Is a Direct HIF-1 Target Gene.** Although previous studies have shown that PDGF-B mRNA expression is regulated by hypoxia and HIF-1 in other cell types (24–26), it was not established whether *PDGFB* is a direct HIF-1 target gene, which requires the identification of a HIF-1–binding site within the context of a functional hypoxia response element. To address this question, we identified seven matches to the consensus HIF-binding site (HBS) sequence 5′-[A/G]CGTG-3′ in the human *PDGFB* gene (HBS1–7; green triangles in Fig. 3*G*). To determine whether HIF-1 binds to any of these sites, we performed ChIP followed by qPCR using primers spanning the putative HIF-1–binding sites. *RPL13A*, which is a gene that is not transactivated by HIF-1, served as a negative control (Fig. S3*A*). ChIP revealed significant DMOG-induced binding of HIF-1α and HIF-1β only to HBS5, which is located in intron 3 of the *PDGFB* gene and contains tandem HIF-1–binding sites (Fig. 3 *G–I* and Fig. S3 *A* and *C*). In contrast, ChIP analysis of DMOG-induced binding of HIF-2α showed no significant enrichment at any of the HBSs studied (Fig. S3*B*). However, HIF-2α binding to the *VEGFA* gene, which served as a positive control, was observed. To determine whether the 39-bp HBS5 sequence is sufficient to regulate hypoxia-induced transcription of a heterologous gene, we constructed luciferase reporter genes containing wild-type HBS5 or a mutant HBS5 in

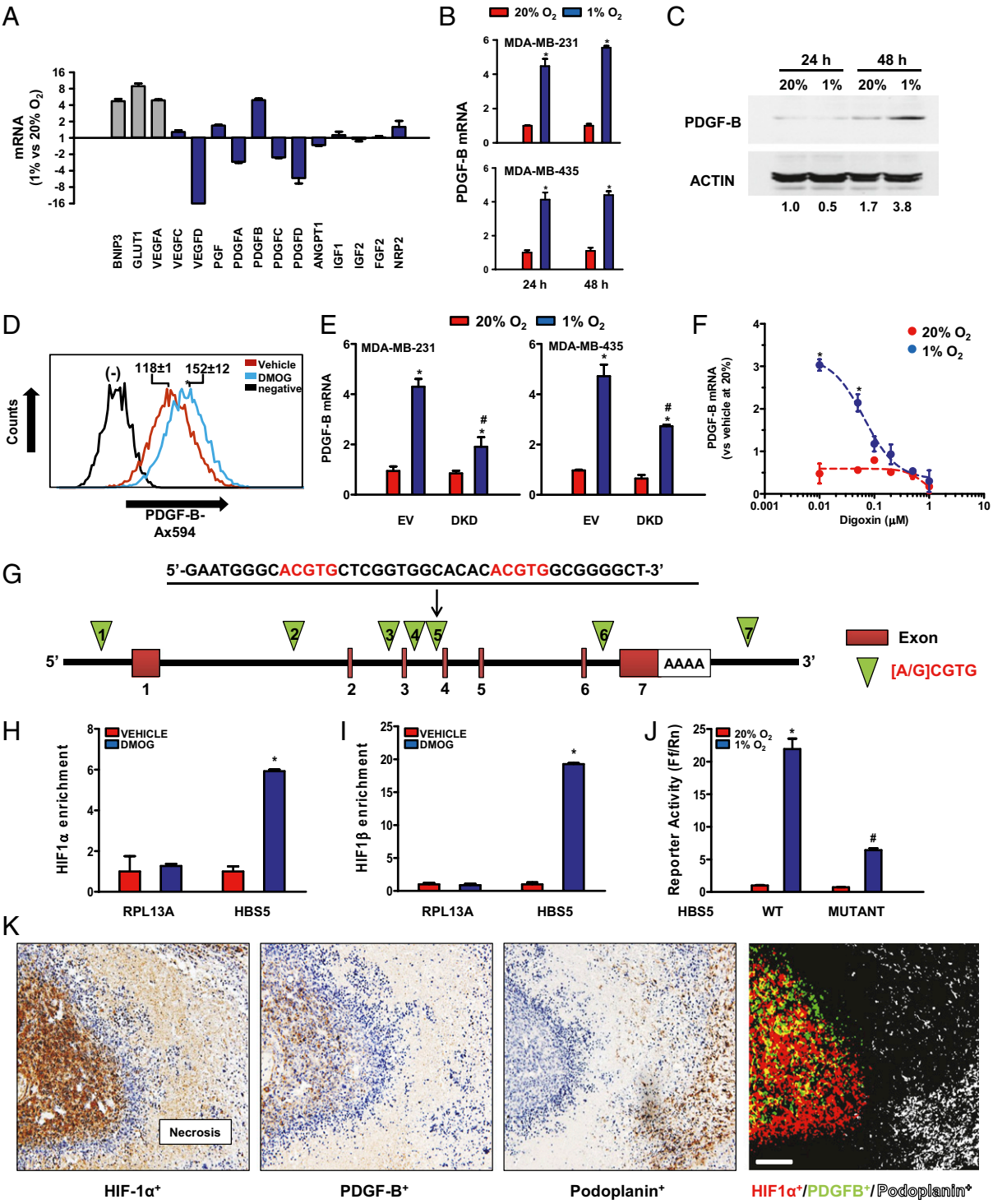

Fig. 3. Hypoxia induces HIF-1–dependent *PDGFB* gene transcription. (*A*) Hypoxia-induced expression of HIF-1–regulated (gray bars) and prolymphangiogenic (blue bars) mRNAs in MDA-MB-231 BCCs; mRNA fold change in cells after 24 h at 1% O_2 relative to 20% O_2 is shown. (*B*) PDGF-B mRNA levels in BCCs after 24 or 48 h at 20% (red bars) or 1% (blue bars) O_2. (*C*) PDGF-B immunoblot assay of MDA-MB-231 BCCs exposed to 20% or 1% O_2 for 24 or 48 h. (*D*) PDGF-B expression after exposure of BCCs to DMOG. Numbers indicate mean fluorescence intensity by flow cytometry. (*E*) PDGF-B mRNA expression in EV and DKD subclones of MDA-MB-231 and MDA-MB-435. (*F*) Effect of digoxin on PDGF-B mRNA expression. (*G*) Location of each candidate HBS in the human *PDGFB* gene. (*H* and *I*) ChIP assay for HBS5 in cells exposed to vehicle or DMOG using HIF-1α (*H*) or HIF-1β (*I*) antibodies. *RPL13A* was used as a negative control. (*J*) Hypoxia response element reporter assay. A wild-type sequence at HBS5 or a mutant sequence containing dual CGT→AAA substitutions was inserted into a firefly luciferase (Ff) reporter and cotransfected with a control Renilla luciferase (Rn) reporter into cells that were incubated at 20% or 1% O_2 for 24 h. The Ff/Rn ratio was calculated and normalized to 20% O_2. (*K*) HIF-1α, PDGF-B, and podoplanin IHC in consecutive sections of an MDA-MB-231 orthograft. Deconvoluted images were pseudocolored to localize HIF-1α$^+$ (red), PDGF-B$^+$ (green), and HIF-1α$^+$PDGF-B$^+$ (yellow) BCCs and podoplanin-positive LVs (white). (Scale bar, 50 μm.) $^*P < 0.001$, 1% vs. 20% O_2 in *B*; $^*P < 0.05$ vs. EV at 20% O_2 and $^{\#}P < 0.05$ vs. EV at 1% O_2 in *E*; $^*P < 0.001$ vs. 20% O_2 at corresponding doses in *F*; $^*P < 0.05$ vs. vehicle in *H* and *I*; $^*P < 0.05$ vs. WT at 20% O_2, and $^{\#}P < 0.05$ vs. WT at 1% O_2 in *J* by Bonferroni test after ANOVA. Data are shown as mean ± SEM (n = 3–4).

which the two 5′-ACGTG-3′ sequences (red in Fig. 3*G*) were replaced by 5′-AAAAG-3′. Luciferase expression in cells transfected with the reporter containing wild-type HBS5 increased 22-fold under hypoxic conditions (Fig. 3*J*), whereas mutation of HBS5 significantly reduced hypoxic induction, demonstrating that HBS5 is a functional hypoxia-response element.

If HIF-1 is critical for PDGF-B expression in vivo, then the proteins should colocalize in breast tumors. To test this hypothesis, we performed immunohistochemical analysis of HIF-1α and PDGF-B protein expression in MDA-MB-231 orthografts using consecutive 5-μm sections; this analysis revealed colocalization of HIF-1α and PDGF-B expression (Fig. 3*K*). Furthermore, HIF-1α$^+$/PDGF-B$^+$ double-positive cells were detected near podoplanin-positive LVs, suggesting a paracrine effect of HIF-1→PDGF-B signaling on lymphangiogenesis.

HIF-1→PDGF-B→PDGFRβ Signaling Enhances LEC Proliferation and Migration. Overexpression of PDGF-B in T241 fibrosarcoma cells promoted lymphatic metastasis by stimulating LEC migration and proliferation (22). To evaluate the paracrine role of PDGF-B expression by BCCs on LVs, we next analyzed the expression of its cognate receptor. PDGFRβ mRNA was expressed in human LECs, and exposure of the cells to 1% O_2 for 48 h increased PDGFRβ mRNA levels by more than fourfold (Fig. 4*A*). Flow cytometry demonstrated PDGFRβ protein on the surface of LECs, and expression levels were increased significantly under hypoxic conditions (Fig. 4*B*). Treatment of LECs with digoxin significantly inhibited the hypoxic induction of PDGFRβ mRNA (Fig. 4*A*). These data suggest that HIF-dependent induction of PDGFRβ may increase the sensitivity of hypoxic LECs to PDGF released from hypoxic BCCs. To demonstrate PDGF-BB→PDGFRβ signaling, LECs were treated with recombinant PDGF-BB protein, which induced phosphorylation of PDGFRβ that peaked at 5–10 min and returned to baseline levels after 15 min (Fig. 4*C*). PDGF-BB–induced phosphorylation of PDGFRβ was decreased significantly when LECs were cotreated with the tyrosine kinase inhibitor imatinib (Fig. 4*D*), as previously reported (5).

To link transactivation of *PDGFB* by HIF-1 in BCCs (Fig. 3) to increased LV density in primary breast tumors (Fig. 2), we investigated whether conditioned medium (CM) from hypoxic BCCs exerts a proliferative effect on LECs. CM from hypoxic EV cells had a greater stimulatory effect on LEC proliferation (assayed by flow cytometry) than did CM from nonhypoxic cells, but this hypoxic induction was lost when DKD cells were used as the source of CM (Fig. 4*E*). The proliferative effect of hypoxic CM on LECs also was lost when EV cells were treated with imatinib (Fig. 4*E*). Hypoxia increases the migration of LECs toward MDA-MB-231 cells (18). LEC chemotaxis was stimulated by hypoxic CM from EV cells but not from DKD cells or EV cells treated with imatinib (Fig. 4*F*). Treatment of EV cells with neutralizing antibody against PDGF-B abrogated the effect of hypoxic CM on LEC proliferation (Fig. 4*G*) and migration (Fig. 4*H*).

To establish definitively the role of PDGF-B expression in the proliferative and chemotactic effect of hypoxic CM from BCCs, we transduced MDA-MB-231 cells with lentivirus encoding an shRNA-targeting PDGF-B (sh576), which blocked the hypoxic induction of PDGF-B by >80% at the mRNA and protein levels (Fig. 4 *I* and *J*). The proliferative effect of CM from hypoxic EV cells was not observed when LECs were exposed to CM from hypoxic sh576 BCCs (Fig. 4*K*). Loss of the chemotactic effect of CM from hypoxic BCCs on LECs also was observed when sh576 cells were assayed (Fig. 4*L*). These results indicate that HIF-1–dependent PDGF-B expression by BCCs mediates the proliferative and chemotactic effects of hypoxic CM on LECs, which is dependent on signaling through PDGFRβ phosphorylation, because it was inhibited by concentrations of imatinib that do not affect VEGF, EGF, or FGF receptor signaling (27, 28).

HIF-1 or PDGFR Inhibition Decreases Tumor Growth, LV Density, and LN Metastasis. Because cell-culture data indicated that HIF-1–mediated PDGF-B expression in BCCs induces proliferation and migration of LECs, we investigated whether inhibition of HIF-1 or PDGFRβ with digoxin or imatinib, respectively, would decrease LV density and LN metastasis after MFP injection of MDA-MB-231 or MDA-MB-435 cells. HIF inhibition by digoxin resulted in a 78% reduction in tumor growth (Fig. 5*A*) and mass (Fig. S4*A*), a 47% reduction in peritumoral LV density (Fig. 5*B*), and a 94% reduction in ipsilateral axillary LN metastasis (Fig. 5*C*). PDGF-B knockdown (Fig. S4*B*) resulted in a 77% reduction in tumor growth and mass compared with EV cells (Fig. 5*D* and Fig. S4*C*), a 46% reduction in LV density (Fig. 5*E*), and a 68% reduction in LN metastasis (Fig. 5*F*). Thus, HIF-1–dependent PDGF-B expression in BCCs contributes significantly to peritumoral LV density and axillary LN metastasis.

Imatinib Decreases LV Density and LN Metastasis Independently of Tumor Mass. Imatinib treatment was shown to decrease LV density in gastric cancer xenografts (21), although effects on LN metastasis were not analyzed. Imatinib reduced the growth of MDA-MB 231 and MDA-MB-435 primary tumors by 52% and 58%, respectively (Fig. 5 *G* and *M*), peritumoral LV density by 60% and 55% (Fig. 5 *H* and *N*), and LN metastasis by 45% and 40% (Fig. 5 *I* and *O*). The effects of imatinib on tumor volume reflected corresponding changes in tumor mass (Fig. S4 *D–G*). To exclude any contribution of decreased primary tumor growth to reduced LN metastasis, we allowed imatinib-treated orthografts to grow to a similar volume as tumors from saline-treated mice (Fig. 5 *J* and *P*). Peritumoral LV density was decreased by 36% and 31% (Fig. 5 *K* and *Q*), and LN metastasis was decreased by 38% and 58% (Fig. 5 *L* and *R*) in MDA-MB-231 and MDA-MB-435 orthografts, respectively. Thus, PDGFR inhibition blocks LN metastasis independently of effects on primary tumor growth. Histopathological analysis revealed the absence of tumor foci in the lungs of the same tumor-bearing mice, suggesting that lymphatic metastasis precedes vascular metastasis in this model (Fig. S5).

HIF-1α and PDGF-B Levels Are Correlated with LV Area and Predict Histological Grade. In light of the evidence from animal studies that HIF-1–mediated PDGF-B expression in BCCs regulates LV density and LN metastasis, we sought to extend these findings to clinical cases of breast cancer. Although a prior study had shown that HIF-1α and PDGF-B expression are associated in breast cancer biopsies, histological colocalization was not investigated (20). We analyzed biopsies of 16 women diagnosed with breast cancer, whose clinical characteristics are summarized in Table S1. IHC for HIF-1α and PDGF-B indicated that BCCs in human invasive ductal carcinoma coexpress HIF-1α and PDGF-B (Fig. 6*A*). Quantitative digital analysis of signal intensity revealed that expression of HIF-1α and PDGF-B was linearly correlated in breast cancer biopsies from patients diagnosed with grade 2 (intermediate differentiation) or grade 3 (poorly differentiated) breast carcinoma, according to the Scarff–Bloom–Richardson histopathological score (Fig. 6*B*) (29, 30). Mean signal intensity increased with histological grade for both HIF-1α (Fig. 6*C*, *Left*) and PDGF-B (Fig. 6*C*, *Right*). We digitally quantified the mean luminal LV area in the same samples subjected to podoplanin IHC (Fig. 6*D*) and found that LV area increased as a function of histological grade (Fig. 6*E*). Given these data indicating that HIF-1α and PDGF-B levels and LV area are correlated with the grade and, therefore, with the progression of human breast cancers, we modeled the interaction among these variables. Multiple linear regression analysis showed that HIF-1α and PDGF-B expression, together with LV area, are linearly correlated and predict the Scarff–Bloom–Richardson histopathological score (Fig. 6*F*). Other factors (tissue area, vessel number, or total

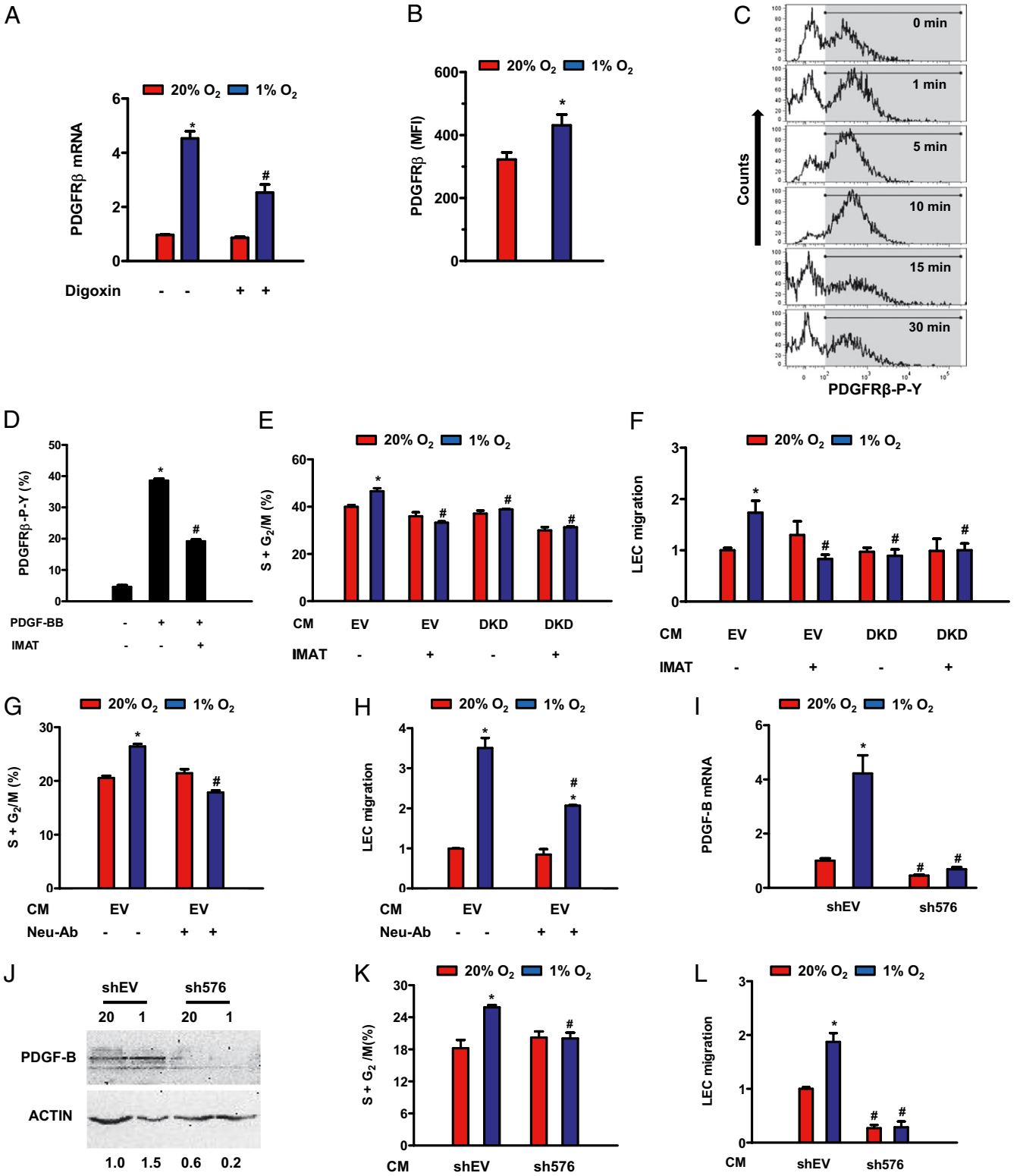

Fig. 4. HIF activity stimulates LEC proliferation and migration. (*A*) PDGFRβ mRNA levels in LECs exposed to 20% or 1% O_2 for 24 h in the presence of vehicle or 50 nM digoxin. (*B*) Surface expression of PDGFRβ on nonpermeabilized LECs as detected by flow cytometry. (*C*) Flow cytometric detection of tyrosine phosphorylated PDGFRβ in LECs incubated with recombinant PDGF-B for the indicated times; gray-shaded area corresponds to positive LECs. (*D–F*) Effect of imatinib treatment (IMAT; 10 μM) on PDGFRβ phosphorylation (*D*), LEC proliferation (*E*), and LEC migration (*F*) induced by CM from EV or DKD BCCs that were incubated under 20% or 1% O_2 for 48 h. (*G* and *H*) Effect of PDGF-B–neutralizing antibody (Neu-Ab) on proliferation (*G*) and migration (*H*) of LECs exposed to CM from EV BCCs incubated under 20% or 1% O_2 for 48 h. (*I* and *J*) PDGF-B expression, as determined by RT-qPCR (*I*) and immunoblot (*J*) assays in BCCs transfected with shRNA against PDGF-B (sh576) or empty vector (shEV) and exposed to 20% or 1% O_2 for 24 h. (*K* and *L*) Effect of CM obtained from shEV or sh576 BCCs incubated under 20% or 1% O_2 for 48 h on LEC proliferation (*K*) and migration (*L*). $^*P < 0.05$ vs. 20% O_2 (*A*, *B*, *E–I*, *K*, and *L*); $^*P < 0.05$ vs. vehicle at 20% O_2 (*D*); $^{\#}P < 0.05$ vs. 1% O_2 or hypoxic CM (*A*, *D*, *E–I*, *K*, and *L*) by Student's *t* test or ANOVA followed by Bonferroni or Holm–Sidak post hoc test. Data are expressed as mean ± SEM ($n = 3–5$).

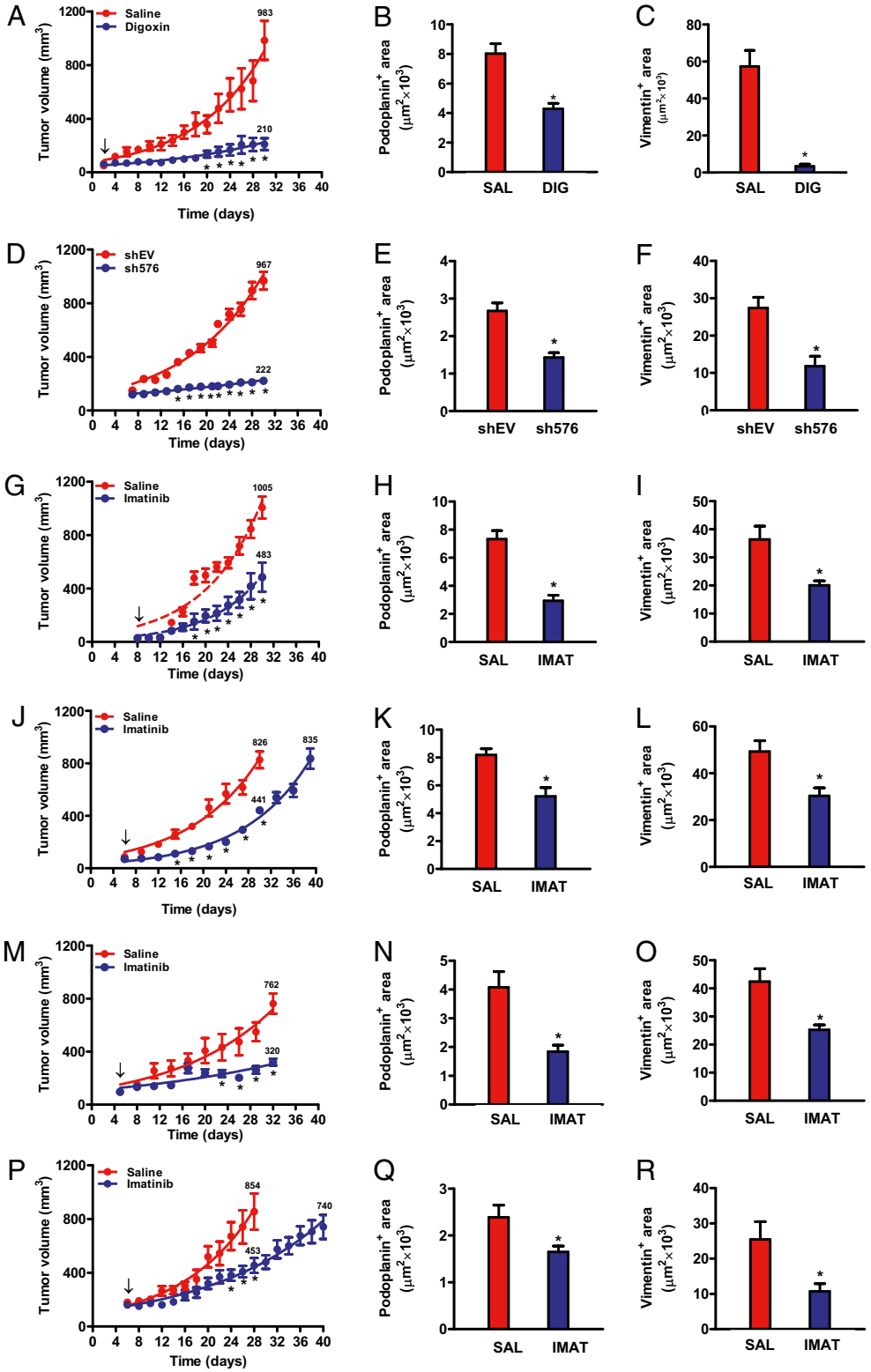

Fig. 5. HIF-1 or PDGF-B inhibition decreases LV area and LN metastasis of BCCs. (*A–C*) SCID mice received MFP injection of MDA-MB-231 cells and were treated with digoxin (blue, DIG) or saline (red, SAL). Serial tumor volumes (*A*), podoplanin-positive peritumoral LV area (*B*), and vimentin-positive area in axillary LNs (*C*) are shown. (*D–F*) MDA-MB-231 cells stably transduced with vector encoding shRNA against PDGF-B (sh576) or empty vector (shEV) were injected into the MFP, and tumor volumes (*D*), podoplanin-positive LV area (*E*), and vimentin-positive LN area (*F*) were determined. (*G–I*) MDA-MB-231 tumor volumes (*G*), podoplanin-positive area (*H*), and vimentin-positive LN area (*I*) were determined in mice treated with imatinib or saline. (*J–L*) MDA-MB-231 orthografts were grown to similar mean volumes (*J*; 830 ± 70 mm^3) for quantification of the podoplanin-positive LV (*K*) and vimentin-positive LN (*L*) areas. (*M–O*) MDA-MB-435 tumor volume (*M*), podoplanin-positive LV area (*N*), and vimentin-positive LN area (*O*) were determined in mice treated with imatinib or saline. (*P–R*) MDA-MB-435 orthografts were grown to similar mean volumes (*P;* 800 ± 48 mm^3) for quantification of podoplanin-positive LV (*Q*) and vimentin-positive LN (*R*) areas. In *A*, *G*, *J*, *M*, and *P*, arrow indicates initiation of drug treatment. *$P < 0.05$ by Student's *t* test or Bonferroni test after two-way ANOVA. Data are expressed as mean ± SEM (n = 5–8).

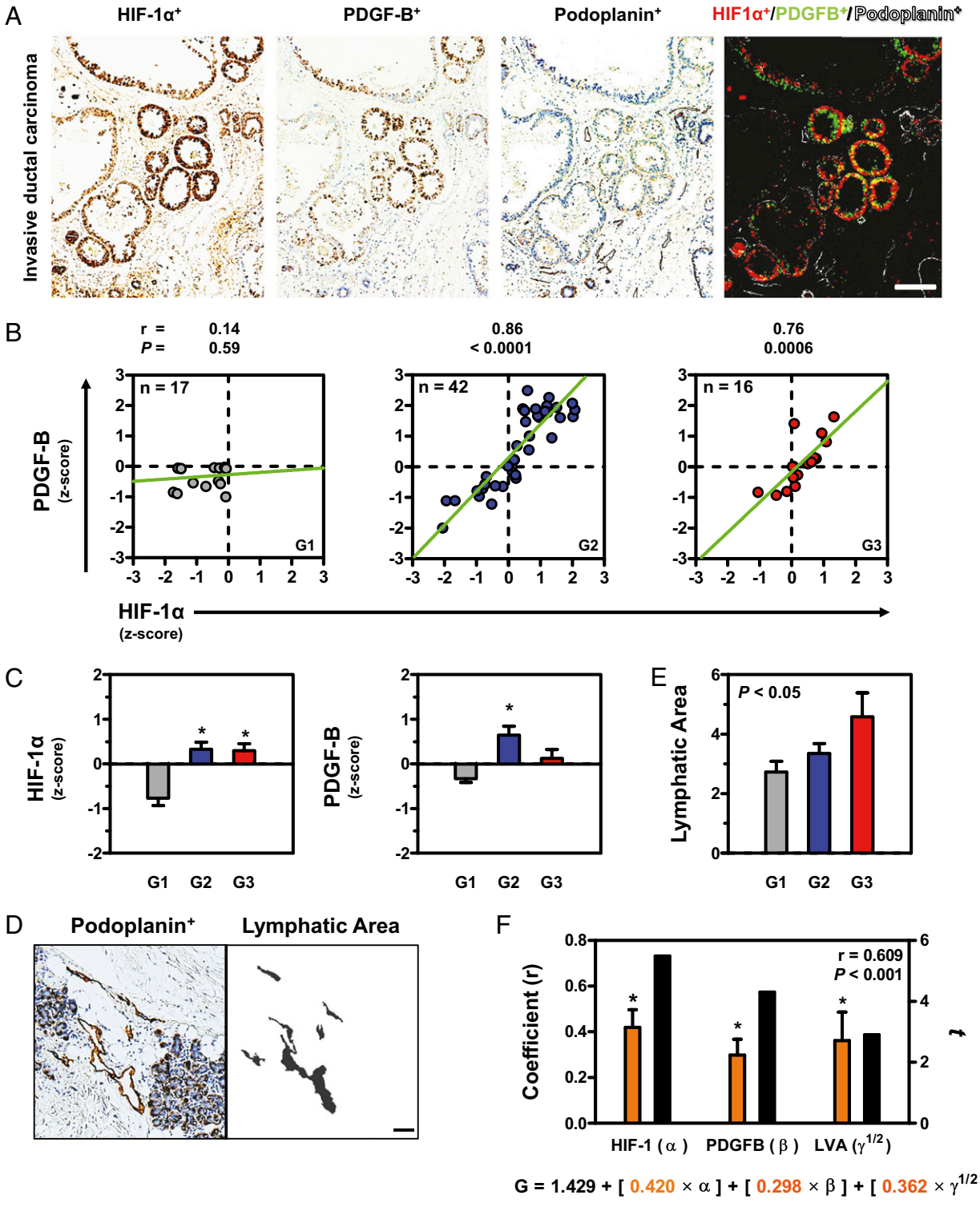

Fig. 6. HIF-1α and PDGF-B expression correlate with LV area and predict histological grade of human breast cancers. (*A*) IHC for HIF-1α, PDGF-B, and podoplanin in biopsy sections from an invasive ductal carcinoma (grade 2). Deconvoluted images were thresholded and pseudocolored for HIF-1α (red), PDGF-B (green), HIF-1α and PDGF-B (yellow), and podoplanin (white). (Scale bar, 500 μm.) (*B*) Linear regression analysis of HIF-1α and PDGF-B staining intensity in grade 1 (G1, *Left*), 2 (G2, *Center*), and 3 (G3, *Right*) breast cancer biopsies. Correlation coefficient (*r*) and *P* values are indicated above each plot. (*C*) Staining intensity *Z*-score for HIF-1α (*Left*) or PDGF-B (*Right*) in biopsies according to histological grade. (*D*) LVs before and after digital deconvolution for podoplanin signal. Photomicrograph (*Left*) shows IHC for podoplanin (brown). Digital image (*Right*) shows luminal LV area (black). (Scale bar, 500 μm) (*E*) Quantification of LV area measured by podoplanin IHC according to histological grade. (*F*) Multiple linear regression analysis of HIF-1α and PDGF-B expression and LV area (LVA). Correlation coefficients for HIF-1α (α), PDGF-B (β), and LVA (γ) are indicated by orange bars (left *y*-axis), whereas the *t* statistic for each coefficient is shown in black bars (right *y*-axis). The three factors were positively correlated with histological grade (G), and the overall linear model equation is shown below the graph (LVA was normalized using a square root transform). *$P < 0.05$ by *F* test or Bonferroni post hoc comparisons after one-way ANOVA. *P* values indicate overall statistical significance. Data are expressed as mean ± SEM.

tissue cell number) were not significant predictors in the model and were eliminated after best-subset regression analysis. Taken together, the data obtained from patient samples are consistent with the animal and cell-culture experiments, indicating that HIF-1→PDGF-B→PDGFRβ signaling plays a critical role in determining LV density and LN metastasis in human breast cancers.

Discussion

Our findings demonstrate the direct involvement of HIFs in the lymphatic metastasis of breast cancer. We identified *PDGFB* as a HIF-1 target gene that is transcriptionally activated in hypoxic BCCs. Genetic HIF or PDGF-B loss of function resulted in decreased LN metastasis and decreased peritumoral LV density. Inhibition of HIF activity or PDGFRβ signaling by treatment of tumor-bearing mice with digoxin or imatinib, respectively, mimicked the effect of genetic knockdown in BCCs by significantly decreasing LV density and LN metastasis. Moreover, we found a strong linear correlation between histological grade, HIF-1α and PDGF-B expression, and LV area in human breast cancer biopsies. HIF-1α and PDGF-B expression were colocalized in 15 of the 16 biopsies analyzed, supporting the clinical implications of our mouse model.

Previous descriptive studies reported correlations between HIF-1α expression and VEGF-C, FGF-2, and PDGF-B in breast cancer (12, 20), gastric carcinoma (21), squamous cell carcinoma (14, 17), and mesothelioma (31). Importantly, HIF-1α levels had prognostic value in LN-negative breast carcinomas (13). However, the molecular mechanisms underlying these clinical observations were not delineated, and it was not known whether HIF inhibition could affect lymphatic dissemination of cancer cells. We show that genetic knockdown of HIF activity in BCCs resulted in tumors with decreased metastasis to axillary LNs in vivo and decreased LEC chemotaxis toward CM from BCCs ex vivo. Peritumoral LV density also was impaired in vivo along with decreased proliferation of LECs in response to CM from BCCs ex vivo, thus demonstrating that HIF activation is critical for lymphovascular dissemination.

Screening of genes encoding lymphangiogenic members of the VEGF, FGF, IGF, and PDGF families revealed that only VEGF-A and PDGF-B expression was induced by hypoxia in MDA-MB-231 and MDA-MB-435 BCCs. Analysis of candidate hypoxia response elements in the *PDGFB* genomic sequence, including a candidate in the 5′-flanking sequence that previously was found to be nonfunctional (25), revealed that HIF-1, but not HIF-2, binds selectively to a site in intron 3 to activate *PDGFB* transcription, thereby delineating the molecular mechanism underlying previous observations of HIF-1–dependent induction of PDGF-B in hypoxic cells (24, 32, 33). Because coexpression of HIF-1α and PDGF-B in BCCs was required to establish the relevance of our findings, we confirmed that PDGF-B$^+$ cells in breast cancer orthografts were also HIF-1α$^+$. In addition, HIF-1α$^+$PDGF-B$^+$ cells were in close proximity to LVs, a result that is consistent with a paracrine effect of PDGF-B on peritumoral LVs. Our data confirm previous chemotactic and proliferative effects of PDGF-B on LECs in addition to the effect of PDGF-B in promoting intratumoral lymphangiogenesis and lymphatic metastasis (22) and indicate that PDGF-B is a major downstream effector of HIF-1 in the stimulation of LECs by hypoxic BCCs. Despite the absence of HIF-2 binding to the *PDGFB* gene, HIF-2α loss of function impaired LN metastasis and lymphangiogenesis in MDA-MB-231 orthografts, suggesting that additional HIF target genes contribute to the lymphatic metastasis of breast cancer cells. VEGF-A stimulates lymphangiogenesis and lymphatic metastasis as well as angiogenesis (34–36). Although VEGF-A expression also was induced by hypoxia in BCCs, genetic knockdown of PDGF-B expression was sufficient to decrease LV density and LN metastasis. However, VEGF-A, as well as VEGF-C and other factors that are constitutively expressed in BCCs, also may contribute to LN metastasis.

Pharmacological inhibition of HIF activity or PDGF signaling using digoxin or imatinib, respectively, decreased primary tumor growth, LV density, and LN metastasis following MFP injection of MDA-MB-231 or MDA-MB-435 cells, which are derived from triple-negative breast cancers that lack expression of the estrogen, progesterone, and HER2 receptors and respond poorly to currently available therapies (37). These data suggest that HIF inhibition and PDGFRβ blockade represent candidate strategies to reduce primary tumor growth and lymphatic dissemination, which in turn should reduce metastatic disease and mortality in breast cancer. Furthermore, we have reported previously that digoxin potently inhibits breast cancer metastasis to the lungs via blood vessels (10, 11). However, the translational implications of the current study should be interpreted with caution, because imatinib also blocks PDGFRβ signaling in vascular pericytes, an effect that impaired vessel stability, increased tissue hypoxia, and facilitated hematogenous metastasis in a 4T1 mouse breast cancer model in which rapid tumor growth occurs, bypassing regional LN dissemination (38). In addition, imatinib is not a specific PDGFRβ inhibitor, because it impairs signaling through other tyrosine kinases in a concentration-dependent manner (27, 28). Thus, imatinib could have countertherapeutic effects in breast cancers that metastasize primarily through the hematogenous route or in late-stage cancers in which lymphatic dissemination already has occurred.

Notably, our clinical data revealed coexpression of HIF-1α and PDGF-B in invasive breast carcinomas, and this coexpression correlated with LV area and histological grade according to the Scarff–Bloom–Richardson scale, which in turn is an important predictor of patient survival and response to chemotherapy (29, 30, 39). Data obtained from patient samples are, by their nature, usually correlative, but they provide important confirmation that the results we obtained from mouse orthograft and cell-culture models are clinically relevant. Taken together, our results suggest a critical role of HIF-1→PDGF-B→PDGFRβ signaling in lymphangiogenesis in intermediate to poorly differentiated invasive breast cancers and warrant additional studies with larger sample sizes to evaluate further the prognostic and therapeutic implications of these findings. Specifically, our results suggest that HIF-1α and PDGF-B coexpression may identify LN-negative breast cancer patients who are at high risk for LN metastasis and might benefit from treatment with drugs targeting one or both of these factors.

Materials and Methods

The following experimental procedures are described in *SI Materials and Methods*: orthotopic transplantation of human breast cancer cells, cell culture, immunoblot assays, reverse transcription and quantitative real-time PCR, flow cytometry and cell-cycle analysis, ChIP, histopathology, immunohistochemistry, analysis of clinical breast cancer specimens, digital image analysis, shRNA expression, migration assay, luciferase reporter assay, and statistical analyses. Clinical characteristics of 16 women diagnosed with breast cancer, whose biopsies were analyzed by immunohistochemistry, are presented in Table S1. The nucleotide sequences of primers that were used for quantitative PCR after reverse transcription of mRNA are presented in Table S2. The nucleotide sequences of primers used for quantitative PCR after chromatin immunoprecipitation are presented in Table S3.

ACKNOWLEDGMENTS. We thank the following colleagues at Johns Hopkins University School of Medicine: Weibo Luo for assistance with genomic analysis, Christopher Cooper for technical advice on flow cytometry, and Karen Fox-Talbot for suggestions on immunohistochemistry. We thank Karen Padgett of Novus Biologicals for providing antibodies against PDGF-B, PDGFRβ, and podoplanin. G.L.S. is the C. Michael Armstrong Professor at Johns Hopkins University School of Medicine and an American Cancer Society Research Professor.

1. Ran S, Volk L, Hall K, Flister MJ (2010) Lymphangiogenesis and lymphatic metastasis in breast cancer. *Pathophysiology* 17:229–251.
2. Mohammed RA, Ellis IO, Elsheikh S, Paish EC, Martin SG (2009) Lymphatic and angiogenic characteristics in breast cancer: Morphometric analysis and prognostic implications. *Breast Cancer Res Treat* 113:261–273.
3. Achen MG, McColl BK, Stacker SA (2005) Focus on lymphangiogenesis in tumor metastasis. *Cancer Cell* 7:121–127.
4. Tammela T, Alitalo K (2010) Lymphangiogenesis: Molecular mechanisms and future promise. *Cell* 140:460–476.
5. Cao Y (2005) Opinion: Emerging mechanisms of tumour lymphangiogenesis and lymphatic metastasis. *Nat Rev Cancer* 5:735–743.
6. Vaupel P, Mayer A, Höckel M (2004) Tumor hypoxia and malignant progression. *Methods Enzymol* 381:335–354.
7. Semenza GL (2012) Hypoxia-inducible factors: Mediators of cancer progression and targets for cancer therapy. *Trends Pharmacol Sci* 33:207–214.
8. Liao D, Corle C, Seagroves TN, Johnson RS (2007) Hypoxia-inducible factor-1α is a key regulator of metastasis in a transgenic model of cancer initiation and progression. *Cancer Res* 67:563–572.
9. Wong CC, et al. (2011) Hypoxia-inducible factor 1 is a master regulator of breast cancer metastatic niche formation. *Proc Natl Acad Sci USA* 108:16369–16374.
10. Zhang H, et al. (2012) HIF-1-dependent expression of angiopoietin-like 4 and L1CAM mediates vascular metastasis of hypoxic breast cancer cells to the lungs. *Oncogene* 31: 1757–1770.
11. Wong CC, et al. (2012) Inhibitors of hypoxia-inducible factor 1 block breast cancer metastatic niche formation and lung metastasis. *J Mol Med (Berl)* 90:803–815.
12. Schoppmann SF, et al. (2006) Hypoxia inducible factor-1α correlates with VEGF-C expression and lymphangiogenesis in breast cancer. *Breast Cancer Res Treat* 99: 135–141.
13. Bos R, et al. (2003) Levels of hypoxia-inducible factor-1α independently predict prognosis in patients with lymph node negative breast carcinoma. *Cancer* 97: 1573–1581.
14. Kurokawa T, et al. (2003) Overexpression of hypoxia-inducible-factor 1α(HIF-1α) in oesophageal squamous cell carcinoma correlates with lymph node metastasis and pathologic stage. *Br J Cancer* 89:1042–1047.
15. Franco M, et al. (2006) Targeted anti-vascular endothelial growth factor receptor-2 therapy leads to short-term and long-term impairment of vascular function and increase in tumor hypoxia. *Cancer Res* 66:3639–3648.
16. Dowlatshahi K, Fan M, Snider HC, Habib FA (1997) Lymph node micrometastases from breast carcinoma: Reviewing the dilemma. *Cancer* 80:1188–1197.
17. Liang X, et al. (2008) Hypoxia inducible factor-α expression correlates with vascular endothelial growth factor-C expression and lymphangiogenesis/angiogenesis in oral squamous cell carcinoma. *Anticancer Res* 28(3A):1659–1666.
18. Mikhaylova M, et al. (2008) Hypoxia increases breast cancer cell-induced lymphatic endothelial cell migration. *Neoplasia* 10:380–389.
19. Koyama Y, et al. (2003) Vascular endothelial growth factor-C and vascular endothelial growth factor-D messenger RNA expression in breast cancer: Association with lymph node metastasis. *Clin Breast Cancer* 4:354–360.
20. Bos R, et al. (2005) Hypoxia-inducible factor-1α is associated with angiogenesis, and expression of bFGF, PDGF-BB, and EGFR in invasive breast cancer. *Histopathology* 46: 31–36.
21. Kodama M, et al. (2010) Expression of platelet-derived growth factor (PDGF)-B and PDGF-receptor β is associated with lymphatic metastasis in human gastric carcinoma. *Cancer Sci* 101:1984–1989.
22. Cao R, et al. (2004) PDGF-BB induces intratumoral lymphangiogenesis and promotes lymphatic metastasis. *Cancer Cell* 6:333–345.
23. Jaakkola P, et al. (2001) Targeting of HIF-α to the von Hippel-Lindau ubiquitylation complex by O_2-regulated prolyl hydroxylation. *Science* 292:468–472.
24. Kelly BD, et al. (2003) Cell type-specific regulation of angiogenic growth factor gene expression and induction of angiogenesis in nonischemic tissue by a constitutively active form of hypoxia-inducible factor 1. *Circ Res* 93:1074–1081.
25. Ullerås E, Wilcock A, Miller SJ, Franklin GC (2001) The sequential activation and repression of the human PDGF-B gene during chronic hypoxia reveals antagonistic roles for the depletion of oxygen and glucose. *Growth Factors* 19:233–245.
26. Zhang SX, et al. (2003) Hypoxia induces an autocrine-paracrine survival pathway via platelet-derived growth factor (PDGF)-B/PDGF-β receptor/phosphatidylinositol 3-kinase/Akt signaling in RN46A neuronal cells. *FASEB J* 17:1709–1711.
27. Buchdunger E, O'Reilly T, Wood J (2002) Pharmacology of imatinib (STI571). *Eur J Cancer* 38(Suppl 5):S28–S36.
28. Buchdunger E, et al. (1996) Inhibition of the Abl protein-tyrosine kinase in vitro and in vivo by a 2-phenylaminopyrimidine derivative. *Cancer Res* 56:100–104.
29. Bloom HJ, Richardson WW (1957) Histological grading and prognosis in breast cancer; a study of 1409 cases of which 359 have been followed for 15 years. *Br J Cancer* 11: 359–377.
30. Amat S, et al. (2002) Scarff-Bloom-Richardson (SBR) grading: A pleiotropic marker of chemosensitivity in invasive ductal breast carcinomas treated by neoadjuvant chemotherapy. *Int J Oncol* 20:791–796.
31. Ohta Y, et al. (1999) VEGF and VEGF type C play an important role in angiogenesis and lymphangiogenesis in human malignant mesothelioma tumours. *Br J Cancer* 81: 54–61.
32. Gleadle JM, Ebert BL, Firth JD, Ratcliffe PJ (1995) Regulation of angiogenic growth factor expression by hypoxia, transition metals, and chelating agents. *Am J Physiol* 268:C1362–C1368.
33. Yoshida D, Kim K, Noha M, Teramoto A (2006) Hypoxia inducible factor 1-α regulates of platelet derived growth factor-B in human glioblastoma cells. *J Neurooncol* 76:13–21.
34. Björndahl MA, et al. (2005) Vascular endothelial growth factor-A promotes peritumoral lymphangiogenesis and lymphatic metastasis. *Cancer Res* 65:9261–9268.
35. Hirakawa S, et al. (2005) VEGF-A induces tumor and sentinel lymph node lymphangiogenesis and promotes lymphatic metastasis. *J Exp Med* 201:1089–1099.
36. Nagy JA, et al. (2002) Vascular permeability factor/vascular endothelial growth factor induces lymphangiogenesis as well as angiogenesis. *J Exp Med* 196:1497–1506.
37. Pal SK, Childs BH, Pegram M (2011) Triple negative breast cancer: Unmet medical needs. *Breast Cancer Res Treat* 125:627–636.
38. Cooke VG, et al. (2012) Pericyte depletion results in hypoxia-associated epithelial-to-mesenchymal transition and metastasis mediated by met signaling pathway. *Cancer Cell* 21:333–345.
39. Elston CW, Ellis IO (1991) Pathological prognostic factors in breast cancer. I. The value of histological grade in breast cancer: Experience from a large study with long-term follow-up. *Histopathology* 19:403–410.